Combined bulk and wall reactions in turbulent pipe flow: decay coefficients and concentration profiles

Kaveh Sookhak Lari, Maarten van Reeuwijk, Čedo Maksimović and Suzan Sharifan

ABSTRACT

This study discusses the effect of combined first-order, bulk and wall reactions on the overall intensity of mass withdrawal in smooth pipes. A one-dimensional model for the transport of high Schmidt number compounds (where the Schmidt number is the ratio of the fluid viscosity to the solute diffusivity) is extended with the effect of a first-order bulk reaction. Profiles of velocity and eddy diffusivity are obtained with a standard high Reynolds number k–ϵ closure in combination with a modified Van Driest wall function. By comparing the results of the 1D model to an analytical asymptotic high Sc approximation, it is shown that the interaction between bulk and wall reactions is very weak. In terms of the decay coefficient, a maximum deviation of 4% is observed for very high bulk demand due to the attenuation of the streamwise solute mass flux. The parameter range for which the concentration profiles can be safely assumed to be uniform, both in the viscous sublayer and in the bulk, is established.

Key words | bulk demand, interaction, turbulent flows, wall demand

Kaveh Sookhak Lari (corresponding author)
Maarten van Reeuwijk
Čedo Maksimović
Suzan Sharifan
Department of Civil and Environmental Engineering,
Imperial College London,
London SW7 2AZ, UK
E-mail: *ksookhak@imperial.ac.uk*

INTRODUCTION

Water contamination in distribution networks is a common problem which sometimes has public health consequences (Geldreich 1996). Craun & Calderon (2001) estimated that 26% of waterborne outbreaks in the USA are due to contamination of the distribution systems. Hunter (1997) reported that 15 out of 42 waterborne outbreaks in the UK between 1911 and 1955 were caused by distribution systems. Contaminants in water distribution systems can occur due to contamination at service reservoirs or poor hygiene practice during repair and maintenance. However, apart from these external factors, the system itself affects the water quality and can be considered as a chemical/biochemical reactor. Dissolved oxygen (DO), natural organic matters (NOMs), microorganisms, residual chlorine, residual coagulants, alkalinity, iron and manganese, biofilm, corrosion and scaling, roughness, pipe material, temperature and different hydraulic regimes are some of the most important factors affecting water quality in a distribution system (Crittenden *et al.* 2005). Therefore, the quality deterioration through the network needs to be taken into account to ensure acceptable water quality at the consumer's tap.

Due to the difficulty of direct monitoring and controlling water quality in the network, water quality modelling has been an important area of water science since 1960 (Trimble 2007). Several water quality models have been developed to predict quality indicators such as residual chlorine throughout the distribution system. Due to the complex interaction of all the mentioned parameters, water quality models contain many assumptions (Rossman *et al.* 1994).

One of the core assumptions of water quality modelling in distribution systems is to treat individual pipes as (streamwise) one-dimensional elements. However, this simplification

doi: 10.2166/hydro.2010.013

may cause errors in modelling. Focusing on turbulent flows, velocity and eddy diffusivity profiles may vary in different directions. In the most ideal case (sufficiently long and smooth pipes), these profiles vary in the wall-normal direction only. Especially for the wall demand problem, this transverse non-uniformity is of extreme importance since the near-wall concentration depends strongly on the eddy diffusivity profile in the viscous sub-layer (Bird *et al.* 2001).

In large-scale problems (like a network), engineers are more interested in the streamwise behaviour of concentration (like the chlorine depletion coefficient throughout the network, which is known as the decay coefficient) rather than the transverse concentration variations. However these streamwise and transverse behaviours are coupled via the eigenvalues therefore affect each other.

Transverse behaviour of the concentration profile is intensively affected by velocity and eddy-diffusivity profiles. As a result, to have acceptable streamwise modelling, the effects of velocity and eddy diffusivity must somehow be considered. In the pipe flow mass transport problem, the transversal velocity and eddy-diffusivity profiles (or their effects) are usually modelled in the form of:

- averaged cross-sectional velocity and effective eddy diffusivity,
- mass transfer coefficients,
- exact velocity and effective eddy-diffusivity profiles.

By assuming that the velocity and eddy diffusivity are constant, the advection–diffusion equation has a solution in terms of Bessel functions (Biswas *et al.* 1993). By calibrating the solution coefficients for different hydraulic regimes and bulk/wall reaction rates, this solution showed acceptable accuracy for the streamwise averaged concentration and total decay coefficient. However, this analytical solution only considered the effective value of eddy diffusivity and, therefore, was not able to determine the near-wall behaviour of the concentration profiles. Additionally, the model had to be calibrated for each specific Schmidt (*Sc*) number (where *Sc* is the ratio of the solute molecular diffusivity to the fluid kinematic viscosity (Bird *et al.* 2001)) and flow regime.

Mass transfer coefficients (k_f (L T^{-1})) are usually implemented to (indirectly) model the effects of unresolved velocity and eddy-diffusivity profiles. This technique is widely used in modelling packages like EPANET (Rossman *et al.* 1994). In the case of stagnant flow Re <1 where $Re = 2\delta U/\nu$ is the Reynolds number and δ, U and ν are the half-pipe/channel width (L), cross-sectional averaged velocity (L T^{-1}) and fluid kinematic viscosity (L^2 T^{-1})), the mass transfer is derived from a constant $Sh = 2$, where Sh is the Sherwood number defined as $Sh = k_f\delta/D$ and D is the molecular diffusivity coefficient (L^2 T^{-1}); therefore the decay coefficient remains constant. For fully developed laminar flow ($Re < 2000$), Sh (and therefore the mass transfer) slightly increases (from the initial value of 3.65) with respect to Re and Sc (Rossman 2000; Mutoti *et al.* 2007).

For the case of turbulent flow, the mass transfer equation implemented in EPANET is derived from the solution to the Graetz problem, which deals with the heat transfer to the fluid in a pipe with constant-temperature (i.e. Dirichlet) wall conditions (Notter & Sleicher 1971). Consequently, modelling packages like EPANET are able to calculate accurate wall concentration and decay coefficients. However, such models are only applicable for high *Sc* compounds like residual chlorine (Sookhak Lari *et al.* 2010). In addition, such models fail to determine concentration profiles.

Sookhak Lari *et al.* (2010) used a one-dimensional profile of velocity and eddy diffusivity to study the first-order wall demand problem which (in contrast to the Graetz problem) is governed by the Robin boundary condition. They presented a simple iterative approach to determine the lowest eigenvalue (i.e. the decay coefficient sufficiently far away from the pipe entrance) and concentration profiles of solutes with arbitrary *Sc*. Additionally, they derived an analytical solution for the high *Sc* asymptotic behaviour. Results were in good agreement with experimental data and the mass transfer coefficient approach, as used in EPANET.

The aim of this paper is to extend the model presented by Sookhak Lari *et al.* (2010) with the effect of first-order bulk reactions. The study is divided into three cases; two asymptotic cases in which one of the two processes (wall or bulk reactions) dominates and a case where the two processes are of similar importance (mixed demand). For each case, decay coefficients and concentration profiles are discussed. In addition, an analytical approximation to the mixed demand decay coefficient (of high *Sc* compounds) is presented in this study. The accuracy of this approximation is compared to the results of the 1D model.

GOVERNING EQUATIONS

A plane-channel geometry (and therefore a Cartesian coordinate system) will be adopted in this study. This geometry is representative for pipe flows since, for sufficiently high *Re*, the viscous wall region in a pipe geometry becomes so thin that the effect of wall curvature can be neglected. Consequently, it can be expected that the pipe and plane channel geometries behave identically for the mass transport problem. This was recently verified by Sookhak Lari *et al.* (2009) who showed that the decay coefficients of both geometries are identical when scaled by the cross-sectional hydraulic radius and therefore the two geometries may be used interchangeably.

Mass transport

For a fully developed turbulent flow in a plane channel with smooth walls, the Reynolds-averaged solute mass transport equation is (Bird *et al.* 2001)

$$u\frac{\partial c}{\partial x}-\frac{\partial}{\partial y}\left[(D+D_T)\frac{\partial c}{\partial y}\right]+k_b c=0 \tag{1}$$

where $u(y)$ and $c(x,y)$ represent Reynolds-averaged streamwise velocity (L T^{-1}) and mass concentration (M L^{-3}), D_T are eddy diffusivity coefficients (L^2 T^{-1}), k_b is the bulk demand parameter (T^{-1}), which characterizes the effect of water quality on bulk demand, and x and y are the streamwise and transverse directions (L). For the y coordinate, the origin $y=0$ is located on the lower wall. Due to the symmetric nature of the problem, the study is restricted to $y=0$ to δ.

For first-order wall demand, the appropriate boundary condition at the wall is of Robin type (Gustafson 1998):

$$D\frac{\partial c}{\partial y}(x,0)=k_w c(x,0) \tag{2}$$

where k_w is the wall demand parameter (L T^{-1}) which characterizes the reaction rate with the pipe surface. At the channel centre, the symmetric plane boundary condition is applicable:

$$\frac{\partial c}{\partial y}(x,\delta)=0. \tag{3}$$

Equation (1) is a linear Partial Differential Equation (PDE) which can be solved by the method of separation of variables (Weigand 2004; Kreyszig 2006). Sufficiently far from the pipe entrance ($x>>0$), the concentration profile can be decomposed as

$$c(x,y)=c_x(x)c_y(y). \tag{4}$$

Here $c_x=\langle c\rangle$ is the cross-sectional averaged concentration function (M L^{-3}), where

$$\langle X\rangle=\frac{1}{\delta}\int_0^{\delta}X dy \tag{5}$$

is the averaging operator and c_y (–) is a radial scaling function, which has the property

$$\langle c_y\rangle=1 \tag{6}$$

By substituting Equation (4) into (1), averaging the result over the cross section and making use of Equation (2), Equation (1) yields to an exact solution of c_x (see Sookhak Lari *et al.* (2010) for details):

$$c_x=c_0e^{-kx} \tag{7}$$

where c_0 is the average concentration at $x=0$. The radial scaling function c_y is governed by a linear, second-order Ordinary Differential Equation (ODE):

$$kuc_y+\frac{d}{dy}\left[(D+D_T)\frac{dc_y}{dy}\right]-k_b c_y=0 \tag{8}$$

$$D\frac{dc_y}{dy}(0)=k_w c_w \tag{9}$$

$$\frac{dc_y}{dy}(\delta)=0. \tag{10}$$

Here $c_w=c_y(0)$ is the relative wall concentration (i.e. the value of the radial scaling function at $y=0$). The constant k in Equations (7) and (8) is the decay coefficient (L^{-1}) and is given by

$$k=\frac{k_w}{r_h}\frac{c_w}{\langle uc_y\rangle}+\frac{k_b}{\langle uc_y\rangle} \tag{11}$$

where r_h is the cross–sectional hydraulic radius. In mathematical terms, k is the lowest eigenvalue of the problem and Equation (11) is the characteristic equation of Equation (8). Although eigenvalues may have a closed-form solution

for simple cases, they are usually determined numerically in complex situations (Weigand 2004). Equation (8) is one of these situations, since u and D_T are non-trivial functions of y. In addition, the Robin boundary condition (Equation (9)) couples $c_w = c_y(0)$ and $dc_y/dy(0)$, which significantly complicates solving the characteristic equation. For such cases, numerical iteration is carried out between the characteristic equation and BVP until the eigenvalue is converged and the boundary condition is satisfied (Weigand 2004). This technique was used to solve Equations (8) and (11) simultaneously (see Sookhak Lari *et al.* (2010) for details).

The decay coefficient k can also be deduced on physical grounds. Indeed, this coefficient is the ratio of mass withdrawal rate and the total mass flux:

$$k = \frac{\oint \phi_w ds + \iint \phi_b dA}{\iint u c_y dA} \tag{12}$$

where ϕ_w and ϕ_b are the wall mass flux and bulk mass withdrawal given by

$$\phi_w = D\frac{dc_y}{dn}, \quad \phi_b = k_b c_y. \tag{13}$$

Here ds and dA are the infinitesimal perimetric and areal elements, respectively, and n is the wall normal direction. Substituting Equation (13) into Equation (12) yields

$$k = \frac{P_h k_w c_w}{A_h \langle u c_y \rangle} + \frac{k_b \langle c_y \rangle}{\langle u c_y \rangle} \tag{14}$$

where A_h and P_h are the cross-sectional hydraulic area and wetted perimeter, respectively. Since $P_h/A_h = r_h^{-1}$, Equation (14) corresponds identically to Equation (11).

By assigning $r_h = 0.5R$ (where R is the pipe radius [L]), Equations (11) and (14) can be applied for a circular cross-sectional geometry (i.e. pipe).

Hydraulics

To solve the mass transport equation, velocity and eddy-diffusivity profiles are required. The simplest way to determine these profiles is to use mixing length theory throughout the entire cross section (Pope 2000). However, in order to have more accurate results in the bulk region, we use a standard high Re k–ϵ closure of the Reynolds-averaged Navier–Stokes (RANS) equations with wall functions. The values given by the wall function at a point located in the log layer ($y^+ = 50$ in this study) are used to define a boundary condition for k and ϵ equations (see, e.g., Pope 2000). A central finite difference scheme is used to discretize the RANS equations.

For high Sc compounds, the near-wall behaviour of the eddy diffusivity is extremely important, because the mass transport in the wall region is diffusion-limited. Theoretical, numerical and experimental studies have shown that $D_T \sim y^3$ for smooth walls (Notter & Sleicher 1971; Grifoll & Giralt 2000; Bird *et al.* 2001). However, standard wall functions, such as the van Driest wall function (e.g. Pope 2000) fail to capture this behavior. This does not influence the hydraulics, but has great consequences for reactions of high-Sc compounds with the wall. Therefore, a modified van Driest wall function is used, which faithfully reproduces $D_T \sim y^3$ near the wall (Bird *et al.* 2001, p 169; Sookhak Lari *et al.* 2010).

A verification of the flow model is shown in Figure 1 where the results are compared against Direct Numerical Simulation (DNS) data of smooth channel flows for $Re_\tau = 642$ and 2003 ($Re_\tau = u_\tau \delta/\nu$, where u_τ is the friction velocity (L T^{-1})) (Iwamoto *et al.* 2002; Hoyas & Jiménez 2006). This is a typical figure for verification of turbulent bounded flow models (Pope 2000; Bird *et al.* 2001). The horizontal and vertical coordinates show distance from the wall in plus units (i.e. $y^+ = yu_\tau/\nu$) and streamwise velocity in plus units (i.e. $u^+ = u/u_\tau$), respectively. The model is in good

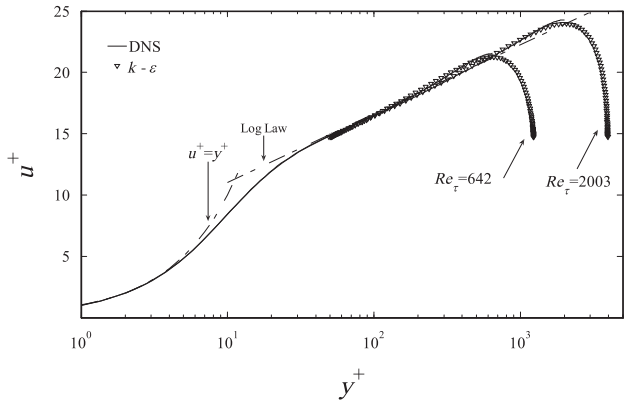

Figure 1 | Verification of the hydraulic model.

agreement with DNS results both in the log layer and the bulk region. Implementing the modified van Driest wall function guarantees implementation of the universal law of the wall throughout the inner layer (Bird *et al.* 2001).

RESULTS AND DISCUSSION

The equation for the decay coefficient k, Equation (11), may be rearranged as

$$k = \frac{k_b}{\langle uc_y \rangle}(\Delta + 1) \tag{15}$$

where

$$\Delta = \frac{k_w}{k_b r_h} c_w. \tag{16}$$

The parameter Δ is the ratio of wall and bulk decay coefficients. The following cases can be distinguished:

$$\begin{cases} \Delta >> 1 \rightarrow \text{Wall demand dominated} & \text{(case 1)} \\ \Delta << 1 \rightarrow \text{Bulk demand dominated} & \text{(case 2)} \\ \Delta \approx 1 \rightarrow \text{Mixed demand} & \text{(case 3)} \end{cases}$$

Sookhak Lari *et al.* (2010) studied pure wall demand (i.e. case 1). In their study, the dependence of the wall decay coefficient on the non-dimensional value k_w/U was evaluated. Their results are briefly discussed in the first part of this section. The second part of this section deals with the pure bulk demand (i.e. case 2). In this part, the dependence of the bulk decay coefficient versus Damkohler (Da) number is evaluated. The latter is the ratio of the bulk demand coefficient to the timescale of the problem (Bird *et al.* 2001):

$$Da = \frac{k_b r_h}{U}. \tag{17}$$

In the last part of this section, the combined bulk and wall demand (i.e. case 3) is studied for different k_w/U and Da. All the cases are studied under the conditions of $Sc = 10^3$ and $Re = 10^5$.

Case 1: pure wall demand ($\Delta >> 1$)

In the absence of bulk demand, the decay coefficient (Equation (11)) takes the form

$$k = \frac{k_w c_w}{r_h \langle uc_y \rangle}. \tag{18}$$

For a high Sc compound, the total mass flux (due to both molecular and eddy diffusivities) remains constant in the viscous sub-layer, and the deviation of concentration profile only takes place in this sub-layer (Garcia-Ybarra & Pinelli 2006; Sookhak Lari *et al.* 2010). Since the thickness of the viscous sub-layer is negligible in comparison to the bulk layer, it is applicable to assume $\langle uc_y \rangle \approx U$. Consequently, Sookhak Lari *et al.* (2010) showed that

$$c_w = \frac{1}{1 + K_W{}^{-1} \frac{k_w}{U}} \tag{19}$$

where

$$K_W = \frac{9\sqrt[3]{b}}{2\pi\sqrt{3}Sc^{2/3}} \frac{u_\tau}{U} \tag{20}$$

is the asymptotic value for kr_h as $k_w/U \rightarrow \infty$ ($b = 9.5 \times 10^{-4}$ in this equation). Substituting Equation (19) into Equation (18), the decay coefficient is given by

$$k = \frac{k_w}{r_h U\left(1 + K_W{}^{-1} \frac{k_w}{U}\right)}. \tag{21}$$

The analytical solution in Equation (21), which was shown to be in good agreement with EPANET and experimental results, is plotted in Figure 2. The asymptotic value of $K_W = kr_h$ is a result of the diffusion-limited characteristic of the wall demand problem. Regardless of the Reynolds number, there is always a very thin layer (adjacent to the wall) inside the viscous sub-layer where the molecular diffusivity dominates the eddy diffusivity. Additionally, the effect of advective mass transport is practically zero in the viscous sub-layer. As a result, the wall demand (or the wall mass flux) is a molecular diffusion-limited process when k_w/U increases and therefore the value of the decay coefficient cannot exceed a certain value (K_w).

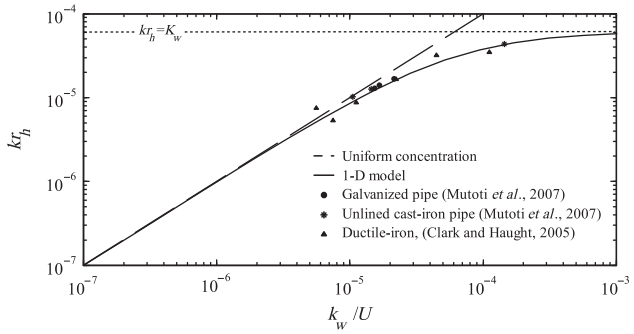

Figure 2 | Analytical pure wall demand decay parameter versus experimental data.

For small k_w/U, a linear relation between k_w/U and kr_h can be discerned. In this region, $c_w \approx \langle c_y \rangle$ and therefore

$$k = \frac{k_w}{r_h U}. \tag{22}$$

This relationship is shown in Figure 2 (uniform concentration line for $Re = 5000$). Clearly, the assumption of uniform concentration holds for $k_w/U < 10^{-6}$ (Figure 2). When $k_w/U > 10^{-6}$, the wall concentration decreases so the wall mass withdrawal ($k_w c_w$) stays in equilibrium with the diffusion-limited mass flux. At this stage, the uniform concentration condition is not valid anymore.

Experimental data of chlorine decay in galvanized and unlined cast iron pipes (Mutoti *et al.* 2007) and ductile iron pipes (Clark & Haught 2005) are shown in Figure 2 as well. The experimental data is reported for a range of Re from 2000 to 8000, and maximum $Da = 5 \times 10^{-7}$ (which is relatively very low in comparison with wall decay coefficients of the data). The reader is referred to the original papers for details of the experiments (diameters, velocities, demand coefficients, test set-up, etc). As can be seen in Figure 2, acceptable agreement is observed between the analytical and real-world data.

The concentration profiles are plotted for different wall demand values in plus units for the viscous sub-layer (Figure 3). Consistent with what was learnt from Figure 2, the wall concentration value is very close to the average concentration for $k_w/U < 10^{-6}$. When k_w/U is larger than 10^{-6}, a significant deviation between wall concentration and $\langle c_y \rangle (= 1)$ is seen. However, the increase in k_w/U only affects the concentration profile in the viscous sub-layer. Regardless of the value of k_w/U, the bulk concentration profile always remains uniform.

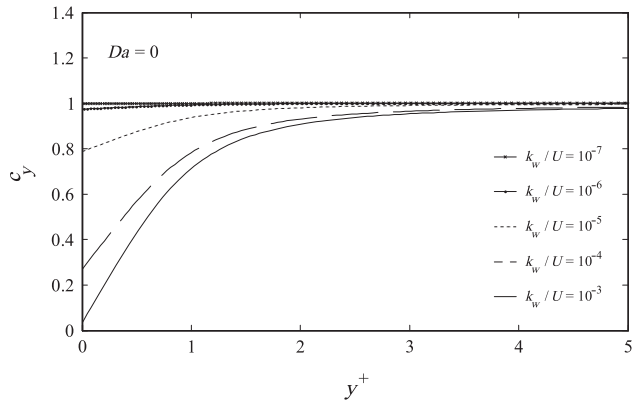

Figure 3 | Concentration profiles for wall demand only ($\Delta \gg 1$).

Case 2: pure bulk demand ($\Delta \ll 1$)

In the absence of wall demand (i.e. $k_w = 0$), the expression for the decay coefficient k (Equation (11)) simplifies to

$$k = \frac{k_b}{\langle u c_y \rangle}. \tag{23}$$

Note that $\langle c_y \rangle = 1$ and therefore does not appear in the numerator. The Robin boundary condition at the wall now changes to a Neumann boundary condition $dc/d_y = 0$. The decay coefficient is plotted versus Da as a solid line (Figure 4), revealing a practically linear relation. Using the approximation $\langle u c_y \rangle \approx U$, Equation (23) is simplified to

$$k = \frac{k_b}{U}. \tag{24}$$

Equation (24) is plotted in Figure 4 by a dashed line. It is observed that Equations (23) and (24) are identical for

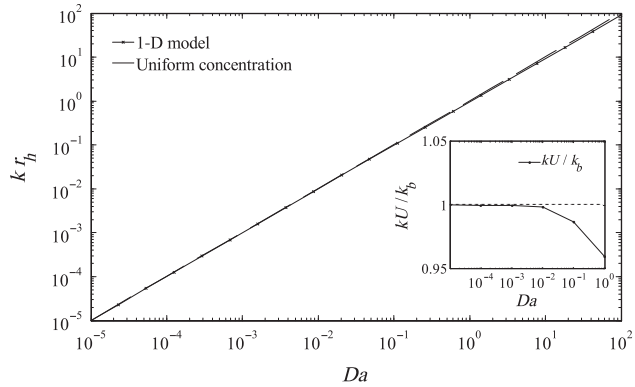

Figure 4 | Pure bulk demand decay parameter (outer plot) and the ratio of the two bulk decay coefficients (inner plot).

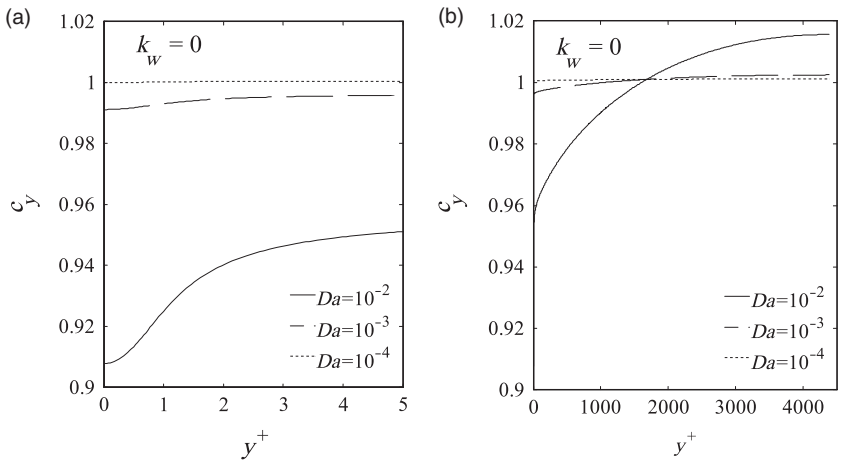

Figure 5 | Concentration profiles for pure bulk demand.

small Da. However, a slight deviation between the two equations can be observed for large Da. In order to study this deviation in more detail, the ratio of the real decay coefficient (k in Equation (23)) to the simplified value of the decay coefficient (k_b/U) is shown in the inner plot of Figure 4. This figure shows that Equations (23) and (24) start to deviate from each other when $Da > 10^{-3}$. However, even at $Da = 1$, the deviation is only 4%. This implies that the assumption of $\langle uc_y \rangle \approx U$ holds for a large range of Da.

Figure 5 shows the concentration profiles at different Da in the viscous sub-layer (a) and bulk regions (b). It is seen that the wall concentration is a function of Da. For $Da < 10^{-3}$, the wall concentration is almost equal to $\langle c_y \rangle$. However, the difference between c_w and $\langle c_y \rangle = 1$ gets larger as Da increases (Figure 5(a)).

Introducing $c_b = c_y(y = \delta)$, Figure 5(b) shows that for $Da < 10^{-3}$, $c_b \approx \langle c_y \rangle = 1$. For $Da > 10^{-3}$, the concentration profile is no longer uniform in the bulk region. It is noted that, regardless of Da, all the concentration profiles coincided with each other at $y^+ \approx 1700$ (Figure 5(b)).

The deviation of c_b and c_w from 1 occurs for $Da > 10^{-3}$, as is shown in Figure 6. Due to the (molecular) limited mixing in the viscous sub-layer, the deviation of c_w increases much faster than c_b (which is located in a region with a much larger eddy diffusivity). The criterion for the concentration uniformity ($c_w = c_b = \langle c_y \rangle$ when $Da < 10^{-3}$) in Figure 6 is consistent with the inner plot of Figure 4 (which shows that the assumption of $\langle uc_y \rangle \approx U$ holds for $Da < 10^{-3}$).

Case 3: mixed demand ($\Delta \approx 1$)

Equation (11) represents the mixed (total) demand decay coefficient. The variation of this decay coefficient versus bulk and wall demands is shown in Figure 7(a, b). The 2D decay coefficient plot (Figure 7(a)) is the projection of the 3D surface plot (Figure 7(b)) on the $kr_h - k_w/U$ plane. For $\Delta << 1$, the value of the decay coefficient converges to the pure bulk decay coefficient (which is shown in Figure 4). Similarly, it is observed that the total decay approaches the pure wall decay (Figure 2) for $\Delta >> 1$.

As a first-order approximation, we can assume that wall and bulk reactions do not influence each other because the former takes place in the viscous sub-layer, whereas the latter mainly takes place in the bulk. This means that the analytical expression for c_w (Equation (19)) is applicable. If, in addition,

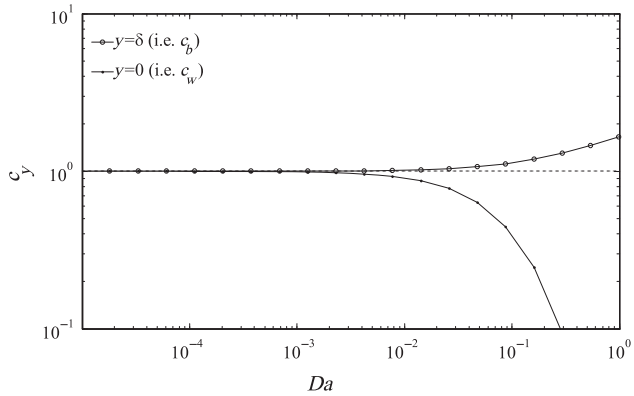

Figure 6 | Variation of wall (c_w) and mid-channel (c_b) concentrations versus Da.

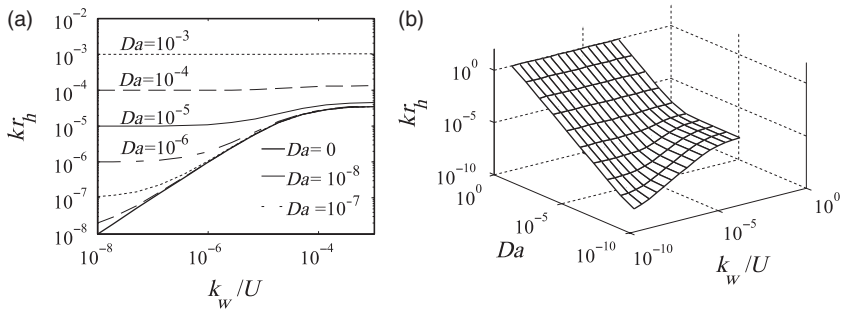

Figure 7 | Mixed demand decay coefficient: (a) 2D plot and (b) 3D plot.

it is assumed that $\langle uc_y \rangle \approx U$, as was done for cases 1 and 2, the following analytical expression is obtained:

$$k_A = \frac{k_b}{U}(\Delta_A + 1). \tag{25}$$

Here

$$\Delta_A = \frac{k_w}{r_h k_b \left(1 + K_W{}^{-1}\frac{k_w}{U}\right)} \tag{26}$$

is an analytical formulation for Δ.

Equation (25) is consistent with the decay coefficient used in the EPANET package. In this package, the wall decay coefficient term (equivalent to $k_b\Delta_A/U$ in Equation (25)) is determined using mass transfer coefficients and the bulk decay coefficient is assigned as in Equation (24) (i.e. k_b/U) (Rossman *et al.* 1994).

To check the accuracy of the analytical approximation (Equation (25)), a normalized error (ϵ) is defined as

$$\epsilon = 100 \times \frac{|k_A - k|}{k}. \tag{27}$$

Equation (27) represents the normalized absolute deviation of the analytical approximation k_A (Equation (25)) from the numerical decay coefficient (Equation (11)). Figure 8 shows contours (isolines) of ϵ. For $Da < 10^{-3}$, the error is negligible. The error slightly increases when Da gets larger than 10^{-3}, the reason for which is that the assumption of $\langle uc_y \rangle = U$ no longer holds. This was discussed in detail in the previous section. Despite some small deviations (maximum error 4%), Equation (25) is a good approximation for the total decay coefficient of high Sc compounds.

The concentration profiles for the mixed demand case are shown in Figure 9. It was found in cases 1 and 2 that wall demand only affects the wall concentration, c_w, while bulk demand affects the entire concentration profile. In the case of mixed demand, both effects occur simultaneously (Figure 9).

When $Da < 10^{-3}$ (the uniform concentration limit for case 2), the concentration profile is only affected by variation of wall demand in the boundary layer (Figure 9(a)). Figure 9(b) shows the boundary layer concentration profiles for $Da = 0.1$. By comparing Figures 9(a) and (b), it is seen that the value of c_w is not only a function of Da but also of k_w. Figure 9(c) clearly demonstrates the bulk concentration profiles for the same Da as in Figure 9(b). The bulk concentration profile is only affected by Da.

Based on the observations so far, a diagram may be constructed for the validity of the assumption of a uniform concentration profile. The results may be categorized with respect to k_w/U and Da. Figure 10 shows different regions for which the uniform concentration assumption is valid or

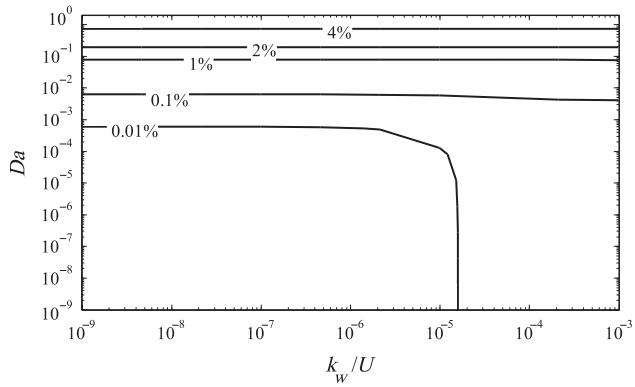

Figure 8 | Error contours of the analytical versus numerical decay coefficient.

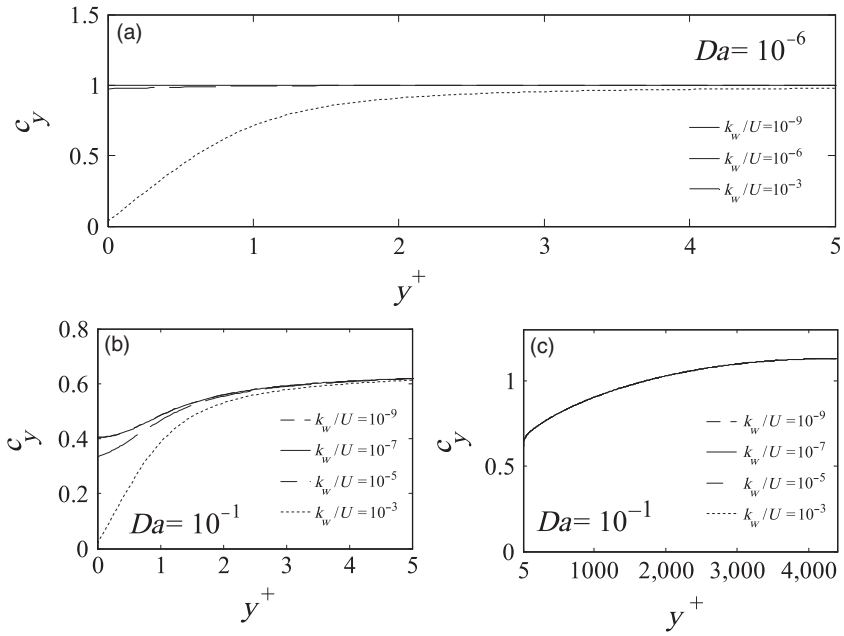

Figure 9 | Concentration profiles of the mixed decay case. (a) Viscous sub-layer close-up at $Da = 10^{-6}$, (b) viscous sub-layer close-up at $Da = 10^{-1}$ and (c) bulk layer at $Da = 10^{-1}$.

violated. For $Da > 10^{-3}$ both wall and bulk layer uniformity assumptions are violated. The boundary layer uniformity stays valid for $Da < 10^{-3}$ and $k_w/U < 10^{-6}$. This assumption is violated for $k_w/U > 10^{-6}$.

CONCLUSION

This paper discussed combined, high *Sc*, first-order wall and bulk reactions in turbulent flows. Using the ratio of wall to bulk demand Δ, three cases could be distinguished: wall demand domination (case 1), bulk demand domination (case 2) and mixed demand (case 3). The analytical form of Δ (Equation (26)), which was obtained using the analytical solution to the wall demand c_w (Equation (19)), provides a good description of all these cases. This implies that the independence of wall and bulk reactions is applicable in the mixed demand problem. The most important findings of these cases are discussed below:

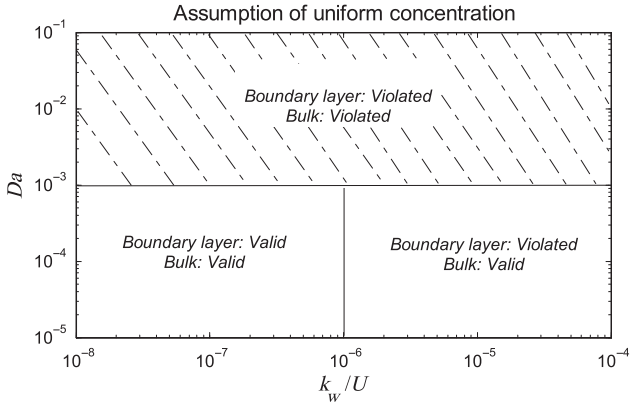

Figure 10 | Concentration uniformity regions of the mixed decay case.

- *Case 1: pure wall demand ($\Delta >> 1$):*
  - Due to the diffusion-limiting property of the viscous sub-layer, the decay coefficient converges to its asymptote (K_W/r_h) when k_w/U increases.
  - The wall demand only affects the viscous sub-layer concentration profile and therefore the assumption of $\langle uc_y \rangle \approx U$ always holds.
  - The concentration profile is uniform when $k_w/U < 10^{-6}$.
- *Case 2: pure bulk demand ($\Delta << 1$):*
  - The decay coefficient is practically a linear function of *Da*.
  - When $Da > 10^{-3}$, the concentration profile becomes non-uniform across the entire fluid layer.
  - The deviation of c_b (for $Da > 10^{-3}$) causes a maximum error of 4% in the assumption of $\langle uc_y \rangle \approx U$ when $Da < 1$.

- *Case 3: mixed demand ($\Delta \approx 1$):*
  - Bulk and wall reactions only very weakly influence each other.
  - Because of the weak influence, an analytical approximation of the decay coefficient is accurate with a maximum deviation of 4% for $Da < 1$.
  - For $Da < 10^{-3}$, the concentration profile is only affected in the viscous sub-layer while both bulk and wall layer concentration profiles are affected for $Da > 10^{-3}$.

This study demonstrated that the assumption of uniform concentration in the bulk region, which is used in packages like EPANET, holds for the first-order reactions in turbulent smooth pipe flows. Several features of the mixed demand case (like independence of the wall and bulk reactions and coinciding of all concentration profiles at $y^+ \approx 1700$) may be used to develop an analytical solution for the mixed demand concentration profiles using matched asymptotic expansions.

Results of this study may give researchers a better insight into the interaction of bulk and wall demand which eventually yields to more accurate simulation packages. The main advantage of the technique presented here is its capability to determine cross-sectional concentration profiles. This advantage is of particular interest when dealing with local reaction rates and by-product formation (such as Disinfection By-Products, (DBPs)). This study may get extended to consider the effect of other flow regimes (stagnant, laminar flow), as well as more complex situations like rough pipe walls, and mixed and higher-order reactions (like biofilm formation).

REFERENCES

Bird, R. B., Stewart, W. E. & Lightfoot, E. N. 2001 *Transport Phenomena*, 2nd edn. John Wiley & Sons, New York.

Biswas, P., Lu, C. & Clark, R. M. 1993 A model for chlorine concentration decay in pipes. *Wat. Res.* **27**(12), 1715–1724.

Clark, R. M. & Haught, R. C. 2005 Characterizing pipe wall demand: Implications for water quality modelling. *J. Wat. Res. Plann. Mngmnt.* 208–217.

Craun, G. F. & Calderon, R. L. 2001 Waterborne disease outbreaks caused by distribution system deficiencies. *J. AWWA* **93**(9), 64–75.

Crittenden, J. C., Trussell, R. R., Hand, D. W., Howe, K. J. & Tchobanoglous, G. 2005 *Water Treatment: Principles and Design*, 2nd edn. John Wiley & Sons, New York.

Garcia-Ybarra, P. L. & Pinelli, A. 2006 Turbulent channel flow concentration profile and wall deposition of large Schmidt number passive scalar. *C. R. Mecanique* **334**, 531–538.

Geldreich, E. E. 1996 *Microbial Quality of Water Supply in Distribution Systems*. CRC Press, Boca Raton, FL.

Grifoll, J. & Giralt, F. 2000 The near wall mixing length formulation revisited. *Int. J. Heat Mass Transfer* **43**, 3743–3746.

Gustafson, K. 1998 Domain decomposition, operator trigonometry, Robin condition. *Contemp. Math.* **218**, 432–437.

Hoyas, S. & Jiménez, J. 2006 Scaling of velocity fluctuations in turbulent channels up to $Re_\tau = 2003$. *Phys. Fluids.* **18**, 11 702.

Hunter, P. R. 1997 *Waterborne Disease: Epidemiology and Ecology*. John Wiley & Sons, Chichester.

Iwamoto, K., Suzuki, Y. & Kasagi, N. 2002 Reynolds number effect on wall turbulence: toward effective feedback control. *Int. J. Heat Fluid Flow* **23**, 678–689.

Kreyszig, E. 2006 *Advanced Engineering Mathematics*, 9th edn. John Wiley & Sons, New York.

Mutoti, G., Dietz, J. D., Arevalo, J. & Taylor, J. S. 2007 Combined chlorine dissipation: Pipe material, water quality and hydraulic effects. *J. AWWA* **99**, 96–106.

Notter, R. H. & Sleicher, C. A. 1971 The eddy diffusivity in turbulent boundary layer near a wall. *Chem. Engng. Sci.* **26**, 161–171.

Pope, S. B. 2000 *Turbulent Flows*. Cambridge University Press, Cambridge.

Rossman, L. A. 2000 *EPANET2 User Manual* EPA/600/R-00/057, United States Environmental Protection Agency (USEPA), Cincinnati, OH.

Rossman, L. A., Clark, R. M. & Grayman, W. M. 1994 Modeling chlorine residuals in drinking water distribution systems. *J. Environ. Engng.* **120**, 803–820.

Sookhak Lari, K., van Reeuwijk, M. & Maksimović, Č. 2009 Is using a plane-channel geometry to model wall-demand in turbulent pipe flow justified? In: *Integrating Water Systems (Proc. 10th International Conference on Computing and Control for the Water Industry, CCWI 2009)*. CRC Press, Boca Raton, FL, pp. 441–445.

Sookhak Lari, K., van Reeuwijk, M. & Maksimović, Č. 2010 Simplified numerical and analytical approach for solutes in turbulent flow reacting with smooth pipe walls. *J. Hydraul. Eng-ASCE.* **136**(9), 626–632.

Trimble, W. 2007 *Encyclopaedia of Water Science*, 2nd edn. CRC Press.

Weigand, B. 2004 *Analytical Methods for Heat Transfer and Fluid Flow Problems*. Springer, Berlin.

First received 8 January 2010; accepted in revised form 18 June 2010. Available online 24 November 2010